Carbon Vol. 18, pp. 313–318
Pergamon Press Ltd., 1980. Printed in Great Britain

SURFACE PROFILOMETRIC STUDY OF THE KINETICS OF THE INTERCALATION OF GRAPHITE†

K. K. BARDHAN

Department of Physics, Carnegie-Mellon University, Pittsburgh, PA 15213, U.S.A.

and

D. D. L. CHUNG

Department of Metallurgy and Materials Science and Department of Electrical Engineering, Carnegie-Mellon University, Pittsburgh, PA 15213, U.S.A.

(*Received* 8 *November* 1979)

Abstract—The kinetics of the intercalation of graphite was investigated by measuring the *c*-face surface profiles during the intercalation of Br_2 into highly-oriented pyrolytic graphite cylindrical discs at room temperature. A sharp intercalate front was observed to advance while the surface profile evolved from a bucket-shape to a V-shape, as predicted by the model of interface-controlled intercalation proposed by the authors [11]. The average magnitude of the steady velocity of the front was ~15 Å/sec; the initial period was marked by a larger velocity attributed to an edge effect. The same behavior was observed during ICl intercalation at room temperature. During desorption, inverted surface profiles were obtained, indicating that desorption may be the reverse of intercalation. In the case of HNO_3 intercalation at room temperature, bowl-shaped surface profiles were observed. Preliminary profile measurements were made during ICl intercalation at 50°C, at which the intercalate layers are known to be disordered.

1. INTRODUCTION

The shape deformation of graphite samples during intercalation is commonly known as the "ashtray effect" or "window pane effect" [1]. Although this effect has been widely observed visually, no systematic investigation of this effect had been previously carried out, except for some measurements of the thickness at the edge and at the center of the *c*-face surface [1]. On the other hand, optical study of the intercalation of lithium in transition metal dichalcogenides [2] had revealed the inward movement of the Li front through the crystal during intercalation, although no quantitative measurement of the movement was made. In this work, the surface topographical profile on the *c*-face was measured during intercalation of highly-oriented pyrolytic graphite (HOPG) in order to elucidate the nature of the deformation and to shed light on the role of strain on the intercalation process, which leads to staging. Elastic effects have been investigated previously in thickness expansion experiments [3, 4], X-ray studies of the carbon–carbon bond length [5], transmission electron microscopy [6], internal friction studies [7] and study of the dependence of the induction period on the mean strain of graphite crystallites [8]. In addition, Hooley has put forward a qualitative strain model [9] and recently there has been a theoretical attempt [10] to explain staging in terms of the elastic interaction. In the earlier paper [11], we presented a phenomenological model of intercalation, which has the elastic interaction as the underlying basis.

Knowledge of the manner in which the dimensions of a sample change during intercalation is important for the analysis of many experimental results, such as those of *in situ* electrical resistivity measurement. Moreover, the shape of the sample can serve as an indicator of the progress of intercalation. Other kinetic studies include measurements of the weight gain, the electrical resistivity and the magnetic susceptibility [12].

2. EXPERIMENTAL

Specimens used in profilometry were all based on highly-oriented pyrolytic graphite (Grade ZYA) kindly provided by Union Carbide Corporation. They were cut into cylindrical discs by using a spark cutter, such that the *c*-axis was parallel to the thickness. Disc diameters vary from 4.5 to 8 mm and disc thicknesses vary typically from ~0.1 to 0.4 mm. Cleaving by using adhesive tape was performed to improve the smoothness of the *c*-face surface. Samples of large thicknesses could not be obtained due to the tendency of splitting during spark cutting.

†Research sponsored by the Air Force Office of Scientific Research Air Force Systems Command, USAF, under Grant No. AFOSR-78-3536. The United States Government is authorized to reproduce and distribute reprints for Governmental purposes notwithstanding any copyright notation hereon.

Profilometry was performed during intercalation with Br_2, ICl and HNO_3, although the intercalation of Br_2 was investigated most extensively. Both intercalation and profilometry were performed at room temperature (22°C), except when mentioned otherwise. Intercalation was achieved by exposing the sample to the saturated vapor of the particular intercalate species. To obtain the variation of the surface profile during intercalation, the sample was removed from the intercalation vessel at regular intervals. Each measurement took typically about half an hour. Occasional interruptions of the intercalation process are believed to have a negligible effect on the experimental results reported here.

The surface profile on the *c*-face was measured with the Tallysurf method by using a surface profilometer (Dektak, Sloan Technical Corp.), which had a diamond stylus of radius 0.0005 in. at the tip. The stylus was allowed to move along several diameters of each disc with a pressure of 50 mg/cm^2, which is fixed by the manufacturer. The maximum range of the profilometer was 0.01 cm, which is, in most cases, less than the maximum expansion possible along the *c*-direction (55% of the sample thickness for the case of Br_2 intercalation). As a result, complete surface profiles during the entire intercalation process could not be obtained.

A smooth surface before intercalation did not necessarily mean that it would remain smooth after intercalation had begun. This was because some graphite flakes on the sample surface became loose during intercalation and caused noise in the profiles. These pieces were carefully removed by means of fine tweezers as much as possible. The randomness of the crystallites about the *c*-axis was strikingly demonstrated by the nearly circular intercalate fronts in circular samples. Another problem was due to the roughness at the edge, which made it impossible to start the profile measurement right at the edge. As a result, the relative value of the edge expansion compared to that of the center could not be obtained from the profile measurement. For simplicity in interpretation, all the samples measured were circular.

We observed that some samples developed ripples near the rim of the *c*-face surface after the start of intercalation. In case of Br_2 intercalation, these samples were not analysed further. However, we found that this phenomenon could not be avoided in ICl intercalation. The cause of this phenomenon is not understood presently.

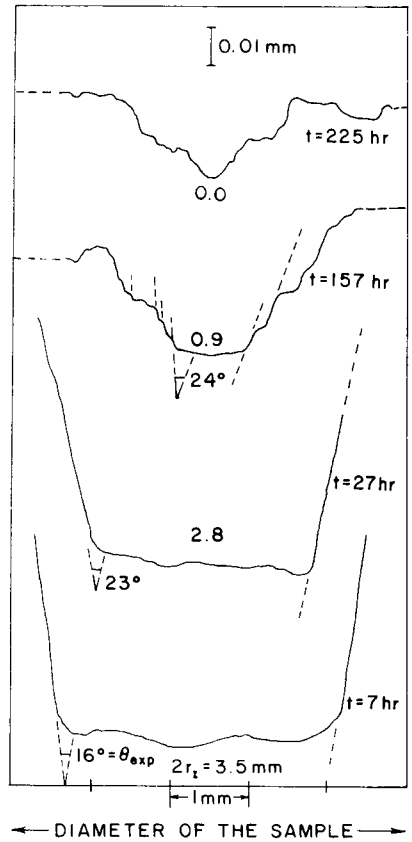

Fig. 1. Sequence of *c*-face profiles of a cylindrical HOPG sample (diameter 4.5 mm, thickness 0.3 mm) as bromination proceeds at room temperature.

Fig. 2. Optical photograph of an HOPG sample (diameter 6.9 mm, thickness 0.1 mm) undergoing intercalation in ICl vapor at room temperature. The sample exhibits a bucket-shaped surface profile on the *c*-face. Note the ripples near the rim of the sample.

3. RESULTS

The evolution of surface profiles during intercalation indicates the existence of two types of profiles. The first type shows a sharp advancing front which delineates an expanded region and an unexpanded region in the early part of intercalation, as observed during intercalation with Br_2 and ICl. The

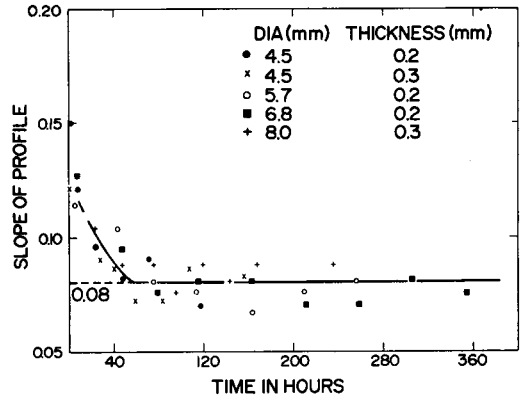

Fig. 3. Plot of the actual slope of the profile vs time for samples of various diameters and thicknesses.

second type does not exhibit any front, but is bowl-shaped throughout the intercalation process, as observed during intercalation with HNO_3.

The sequence of surface profiles of the first type obtained at four different times during Br_2 intercalation is shown in Fig. 1. The sample was of diameter 4.5 mm and thickness 0.3 mm. An advancing intercalate front was clearly observed. In the early part of intercalation, the profile was bucket-shaped. An optical photograph of a sample (diameter 6.9 mm, thickness 0.11 mm) with a bucket-shaped surface profile during ICl intercalation is shown in Fig. 2. Later the profile became V-shaped such that the region outside the V-shaped part of the profile was roughly flat. As intercalation further progresses, the V-shaped part of the profile decreases in size and eventually leaves a rough flat surface.

Of importance is the linearity of the slanted portions of the profile, i.e. the sides of the "bucket". The angle between these sides is indicated for three profiles in Fig. 1. Due to the difference in scale between the vertical and horizontal axes in Fig. 1, the measured angles indicated in Fig. 1 are not the actual angles. Corresponding to the measured angle θ_{exp} (Fig. 1), the actual slope of the slanted portion is 1/50 cot $(\theta_{exp}/2)$. The trend in slope variation, as shown in Fig. 1, is quite representative. This is also shown in Fig. 3, where the actual slope is plotted against the time of intercalation for samples of different diameters and thicknesses. In spite of the scatter in the data points, it is evident that the slope is steep at the beginning and then decreased quickly to a steady value. It should also be noted that the large scatter in the slope data obscures the effect of the size of the sample, if the effect is at all present. The steady value of the slope is about 0.08. Extrapolation to zero time is quite uncertain, given the time scale shown in Fig. 3.

An interesting feature is the appearance of rings, as seen visually, and of corresponding ledges, as seen in the profiles (e.g. at $t = 157$ hr in Fig. 1) after some time of intercalation. In many cases, the parallel nature of the ledges is remarkable and simplifies the determination of the slope, as illustrated by the dashed lines in the third profile from the bottom of Fig. 1. The number of occurrence of the ledges appears to increase with time, but decrease with increasing sample diameter. Moreover, it is insensitive to the thickness. Although the height of the ledges tends to increase with diameter, the width apparently is independent of size and is of the order of 100–150 μm. The origin of the ledges is presently not clear.

The variation in the diameter of the contour of the intercalate front during intercalation is shown in Fig. 4 for samples of different diameters, but of the same thickness, and is shown in Fig. 5 for samples of different thicknesses, but of the same diameter. The slope of this plot yields the velocity of the front. The general features of this plot are noted below.

(1) Each curve is dominated by a linear portion which indicates that the velocity is constant for the most part of the intercalation process. However, the initial portion is characterized by a steeply falling

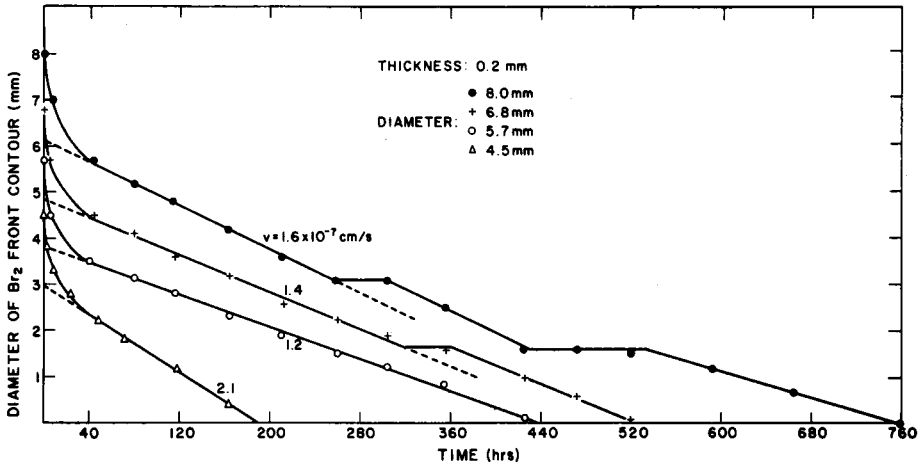

Fig. 4. Plot of the Br_2 front contour diameter vs time for samples of the same thickness but of different diameters. The magnitude of the steady velocity is indicated for each curve.

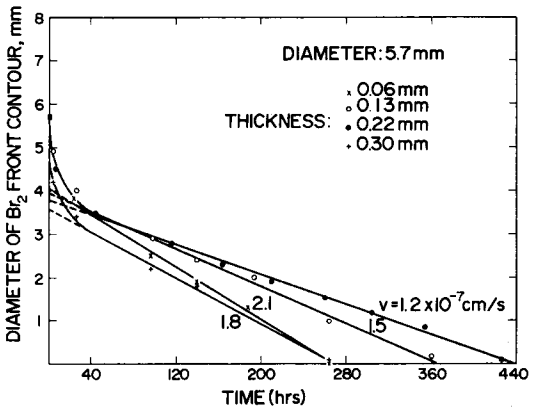

Fig. 5. Plot of the Br_2 front contour diameter vs time for samples of the same diameter but of various thicknesses. The magnitude of the steady velocity is indicated for each curve.

curve, implying that the velocity decreases rapidly from an average initial large value ($\sim 5 \times 10^{-6}$ cm/sec) to a steady value which is at least an order of magnitude less. The magnitude of the steady velocity is shown for each curve.

(2) Irrespective of diameter or thickness, all the curves approach linearity at approximately the same time ($\sim$44 hr), which is close to the time at which the slope becomes steady (Fig. 3). Moreover, the amount of decrease in the intercalate front contour diameter ($\sim$2.3 mm) in this period is apparently independent of the sample diameter or thickness.

(3) There is apparently no correlation between the magnitude of the steady velocity and the sample thickness (Fig. 5). For a given thickness (Fig. 4), the steady velocity appears to be fairly independent of the diameter, as long as the sample diameter is large compared to $\sim$2.3 mm. However, as the diameter becomes comparable to 2.3 mm, as for the 4.5 mm diameter case, the steady velocity increases with decreasing diameter, though the applicable region decreases in extent.

(4) In Fig. 4, the two curves corresponding to large diameters for the same thickness show "steps" (drawn as a guide to the eyes), whereas the other two curves corresponding to smaller diameters do not. As seen in Fig. 5, for the same diameter, no steps appear as the thickness increases.

An interesting conjecture about the last mentioned feature is that, as the sample diameter increases, the steps may become more numerous so as to cause considerable decrease in intercalate absorption rate. The step may even assume an indefinite width so that intercalation stops. It is interesting to note contrasting effects of the diameter and thickness found by Hooley [4] in the intercalation of natural graphite flakes of dimensions generally smaller than those used in this work.

Surprising results were obtained when profilometry was carried out on one of the graphite–Br_2 samples (diameter 5.7 mm, thickness 0.2 mm) during desorption in air from saturation, as shown in Fig. 6. The sequence shown in Fig. 6 is similar to one in Fig. 1, except that each profile is inverted as if desorption is just the reverse mechanism of intercalation. This idea has been previously mentioned by Hooley [9] on the basis of the similarity of isotherms obtained during intercalation and during desorption. Further profilometry work during desorption is in progress in order to obtain a detailed understanding of the mechanism of intercalate desorption.

Similar results were obtained in preliminary profile measurements carried out during vapor phase intercalation of ICl at room temperature. The relatively large expansion during ICl intercalation made the surface topographical features more pronounced than those observed during Br_2 intercalation. The average slope is $\sim$0.1, compared to the value of 0.08 for Br_2 intercalation. Crack formation during ICl intercalation caused considerable experimental problem. This problem could possibly be avoided by using a lower ICl vapor pressure, such as that provided by a solution of ICl in CCl_4. However, this possibility was not pursued further in the present work.

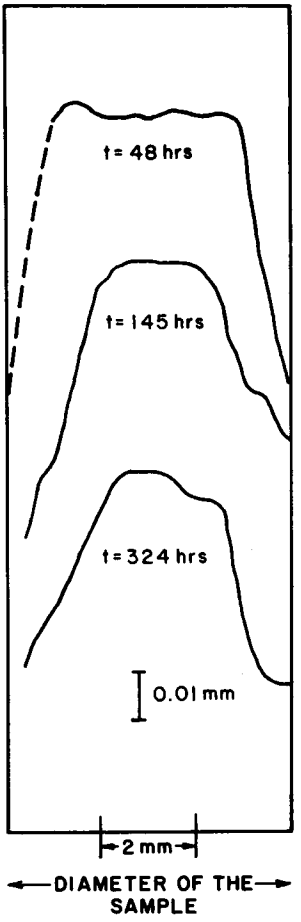

Fig. 6. Sequence of *c*-face profiles during the desorption of a saturated graphite–Br_2 sample (diameter 5.7 mm, thickness 0.2 mm) in air.

It was suggested in the earlier paper [11] that the mechanism of intercalation depends on the intercalation temperature relative to the intralayer order–disorder transformation temperature. Consequently the surface profile also has this temperature dependence. In particular it was suggested that, above the transformation temperature, the surface profile is of the second type. In order to test the validity of this suggestion, intercalation of graphite in saturated ICl vapor at ~50°C was carried out, since the transformation temperature is known to be 41°C for graphite–ICl [13]. The surface profiles obtained were not of the first type, which corresponds to interface-controlled intercalation, in contrast to the corresponding results obtained at room temperature. There was no evidence of a sharp intercalate front. On the other hand, the whole sample was observed to be bent near the edge and therefore was not symmetrical with respect to the middle basal plane. There were visible cracks which are believed to distort the surfaces considerably. As a result, the profiles were not analysed further. It should be mentioned that the absence of a sharp front could not be due to cracks because at room temperature the front was observed, even when there were visible cracks.

Graphite nitrate has disordered intercalate layers at room temperature [14], so we also performed surface profilometry during intercalation of concentrated fuming nitric acid at room temperature. A regular sequence of profiles were obtained, although they were modified by crack formation which was present in various degrees of severity in all the samples investigated. The intercalated samples were curved and the two *c*-face surfaces were not symmetrical. The convex side was inflated like an "air bag", presumably due to cracks. On the contrary, the concave side appeared to be relatively rigid. A profile of this side of a sample of diameter 8.0 mm and thickness 0.25 mm after 4 hr of intercalation is shown in Fig. 7. The bowl-shaped nature of the profile is clear and is believed to be genuine in spite of the modification by cracks. This observation provides experimental evidence of the profile of the second type. The bowl-shape eventually gave way to a rough flat surface when intercalation was completed. The angle shown in Fig. 7, although questionable in its validity, is possibly an indication of the order of magnitude of the rate parameters involved. As in the case of Br_2 intercalation, rings were observed and corresponding steps can be seen in Fig. 7.

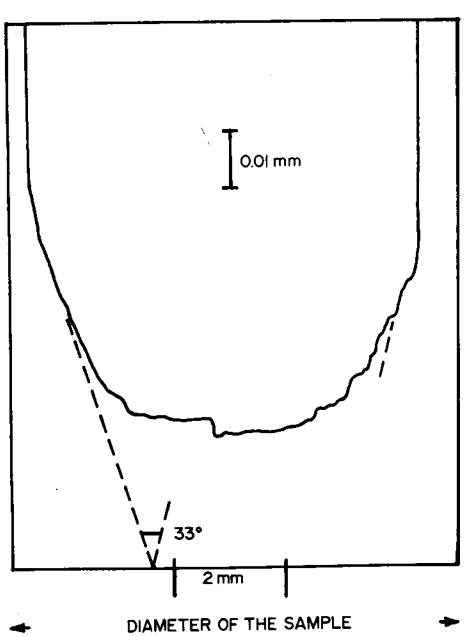

Fig. 7. Surface profile of a graphite–HNO_3 sample (diameter 7.0 mm, thickness 0.24 mm) at room temperature after 4 hr of intercalation.

4. DISCUSSION

It is evident that the surface profile measurements describe rather vividly the kinetics of deformation accompanying intercalation. The results provide us much insight into the mechanism of intercalation. Results are analyzed basically within the framework of the model of first intercalation presented in Ref. [9]. According to the terminology used in the model, profiles of the first type are explained by the interface-controlled mechanism; those of the second type are not discussed further in this paper.

We shall first discuss profiles of the first type as obtained during intercalation with Br_2 or ICl at room temperature. The evolution of surface profiles as predicted for Case 1 of the model of interface-controlled intercalation is in excellent qualitative agreement with the experimental results in Fig. 1. In particular, the change of a "bucket" shape to a "V" shape, as discussed in the model, is well confirmed. All experimental results belong to Case 1, in which the time of nucleation of all layers (t_N) is less than the time of completion of the outermost layers. This is not unexpected in view of the fact that the samples used had the thickness much less than the diameter.

As indicated already in Figs. 3–5, the slope of the profiles and the velocity of the intercalate front remain constant for the most part of the growth period, as was assumed in the model. However, the initial period is apparently marked by changing slope and velocity. This can possibly be attributed to an edge effect for the following reasons. The fact that the velocity decreases from a large value at the edge to a smaller steady value after the intercalate layers have moved a certain distance inside the sample is consistent with a smaller resistance to deformation at the edge than inside. Moreover the distance the intercalate front moves inside until the steady state is reached is independent of the sample diameter. This means that steady state can be considered to correspond to an infinite sample. To take a different point of view, we can consider this observation to provide support for the "two-stage" process of

intercalation [15]—first stage being dominated by the edge effect and the second stage being dominated by the steady-state behavior.

Since, in the model, the slope is equal to $d'/v\Delta T$, where d' is the expansion of the graphite layer spacing and ΔT is the time gap between the formation of two successive intercalate layers, it might seem that the initial decrease in slope may be explained by an increase in ΔT with time. However, the explanation might be applied only up to time t_N, which is also the time required for completing the edge expansion. For the HOPG samples used in the present work, t_N is of the order of a few minutes [16], whereas the slope continues to decrease until a much longer time ($\sim$44 hr). Alternatively, the simple assumption of constant ΔT, with the velocity of growth of the intercalate layers decreasing with increasing distances from the surfaces, can explain the decrease in slope. Indeed, it is quite reasonable to assume that the further away from the c-face surface an intercalate layer is, the smaller is the velocity due to the increasing rigidity before the steady state is reached. Since the time of the first measurement is a few hours after the start of intercalation, a rigorous determination of the parameter ΔT used in the model cannot be made. This is because the determination of ΔT requires the evaluation of the slope by extrapolation to zero time. Due to the scatter in the data, this extrapolation is quite rough. However, this difficulty does not necessarily exist in case of samples which have large values of t_N. It must be noted that using the value of the steady slope yields only a redefined value of ΔT, which is about 3 sec, as compared to the value of 10^{-3} sec obtained from edge expansion results [16].

Acknowledgements—The authors acknowledge the Center for the Joining of Materials of Carnegie-Mellon University for providing the Dektak surface profilometer in its Surface and Micro Analysis Central Research Facility. They are grateful to Union Carbide Corporation for providing the highly-oriented pyrolytic graphite material. They also wish to thank Mr. S. H. Anderson of Carnegie-Mellon University for valuable discussion, particularly regarding the edge effect, and for taking the optical photograph of the graphite-ICl sample and for bringing Ref. [2] to our notice.

REFERENCES

1. A. G. Saunders, Ph.D. Thesis. University of London (1962).
2. R. R. Chianelli, *J. Crys. Gr.* **34,** 239 (1976).
3. J. G. Hooley, W. P. Garby and J. Valentin, *Carbon* **3,** 7 (1965).
4. J. G. Hooley, *Carbon* **10,** 155 (1972).
5. D. E. Nixon and G. S. Parry, *J. Phys. C.* **2,** 1732 (1969).
6. M. Heerschap, P. Delavignette and S. Amelinckx, *Carbon* **1,** 235 (1964).
7. T. Tsuzuku and M. Saito, *Japan J. Appl. Phys.* **6,** 54 (1967).
8. M. B. Dowell, *Mater. Sci. Engng* **31,** 129 (1977).
9. J. G. Hooley, *Chem. Phys. Carbon.* **5,** (1969).
10. S. A. Safron and D. R. Hamann, *Phys. Rev. Lett.* **42,** 1610 (1979).
11. K. K. Bardhan and D. D. L. Chung, *Carbon* **18,** 303 (1980).
12. See references in Ref. [11].
13. J. S. Culik and D. D. L. Chung, *Mater. Sci. Engng* **37,** 213 (1979).
14. D. E. Nixon, G. S. Parry and A. R. Ubbelohde, *Proc. R. Soc. (London)* **A291,** 324 (1966).
15. J. A. Barker and R. C. Croft, *Aust. J. Chem.* **6,** 302 (1953).
16. K. K. Bardhan, S. H. Anderson and D. D. L. Chung, to be published.